Molecular Electronics

Deutsche Ausgabe: DOI: 10.1002/ange.201506458
Internationale Ausgabe: DOI: 10.1002/anie.201506458

Three-State Single-Molecule Naphthalenediimide Switch: Integration of a Pendant Redox Unit for Conductance Tuning

Yonghai Li, Masoud Baghernejad, Al-Galiby Qusiy, David Zsolt Manrique, Guanxin Zhang, Joseph Hamill, Yongchun Fu, Peter Broekmann, Wenjing Hong, Thomas Wandlowski, Deqing Zhang,* and Colin Lambert**

Abstract: *We studied charge transport through core-substituted naphthalenediimide (NDI) single-molecule junctions using the electrochemical STM-based break-junction technique in combination with DFT calculations. Conductance switching among three well-defined states was demonstrated by electrochemically controlling the redox state of the pendent diimide unit of the molecule in an ionic liquid. The electrical conductances of the dianion and neutral states differ by more than one order of magnitude. The potential-dependence of the charge-transport characteristics of the NDI molecules was confirmed by DFT calculations, which account for electrochemical double-layer effects on the conductance of the NDI junctions. This study suggests that integration of a pendant redox unit with strong coupling to a molecular backbone enables the tuning of charge transport through single-molecule devices by controlling their redox states.*

Functional molecules with bi-/multistable states have been intensively studied,[1] because of their potential as building blocks for molecular-level electronics[2] and ultrahigh-density storage devices.[3] Various switchable molecules were fabricated by incorporating photochromic or redox-active moieties within the molecular charge transport pathway, for example, tetrathiafulvalene (TTF),[4] benzodifuran (BDF),[5] anthraquinone (AQ),[6] and ferroence.[7] In these studies, the functional unit was located in the charge-transport pathway, which is expected to provide significant tuning of single-molecule conductance. On the other hand, single-molecule devices with pendant functional units (Figure 1 a), which are not directly involved in the charge-transport pathway, are also of great interest because it offers much more flexibility for molecular design and synthesis, and therefore, finer tuning of the charge transport through the single-molecule device.[8]

Naphthalenediimide (NDI) has attracted much attention in the organic electronics[9] and supramolecular chemistry[10] communities as it acts as an electron acceptor with n-type semiconductor characteristics. Substitution of the naphthalene core provides the opportunity to study charge transport through the naphthalene unit, while the diimide unit serves as a pendant functional unit with strong coupling to the naphthalene backbone and sensitivity to external stimuli, such as applied electrochemical gating. By tuning the potential applied, a sequence of two sequential electron-transfer reactions transforms the neutral species (NDI-N) into the radical anion (NDI-R), and finally into the dianion species (NDI-D). Therefore, the core-substituted NDI molecule can be considered as a prototypical molecular junction for evaluating the effect of pendant redox groups on single-molecule conductance.

Herein, we report an electrochemically controlled scanning tunneling microscopy (STM) based break-junction (BJ) study[6] of an NDI-BT molecule with a pendant diimide redox unit that is strongly coupled to the molecular backbone. We demonstrate that reversible redox transitions in the pendant diimide unit do indeed cause pronounced changes in charge transport through the single molecular NDI-BT junction. To elucidate the microscopic mechanism of electrochemical gating, we employed density functional theory (DFT) to model the charge double layer in the molecular junction formed from ions in the supporting electrolyte, and computed the electrical conductance as a function of the NDI-BT redox states, by using the non-equilibrium Green's function (NEGF) method.

The design of NDI-BT is based on the following considerations: i) NDI can be reversibly transformed into the respective radical anion and dianion with distinguishable energy gaps, ii) the presence of a dihydrobenzo[*b*]thiophene anchor group enables NDI-BT to be contacted to source/drain electrodes (Figure 1 b),[11] and iii) the presence of triple carbon–carbon bonds introduces a certain rigidity into the NDI-BT (the synthesis and UV/Vis absorption spectra of the three charge states are shown in the Supporting Information).

The NDI-BT assembly was prepared on an Au(111) substrate by drop-casting 30 μL of a solution of 0.5 mM NDI-

[*] Dr. Y. Li,[+] Prof. Dr. G. Zhang, Prof. Dr. D. Zhang
Organic Solids Laboratory
Institute of Chemistry, Chinese Academy of Sciences
Beijing 100190 (China)
E-mail: dqzhang@iccas.ac.cn
M. Baghernejad,[+] J. Hamill, Dr. Y. Fu, Dr. P. Broekmann, Prof. Dr. W. Hong, Prof. Dr. T. Wandlowski
Department of Chemistry and Biochemistry
University of Bern
Freiestrasse 3, 3012 Bern (Switzerland)
Prof. Dr. W. Hong
Department of Chemical and Biochemical Engineering
College of Chemistry and Chemical Engineering
Xiamen University, Xiamen 361005 (China)
E-mail: hong@dcb.unibe.ch
A.-G. Qusiy,[+] Dr. D. Zsolt Manrique,[+] Prof. Dr. C. Lambert
Department of Physics, Lancaster University
Lancaster LA1 4YB (UK)
E-mail: c.lambert@lancaster.ac.uk
[+] These authors contributed equally to this work.

Supporting information for this article is available on the WWW under http://dx.doi.org/10.1002/anie.201506458.

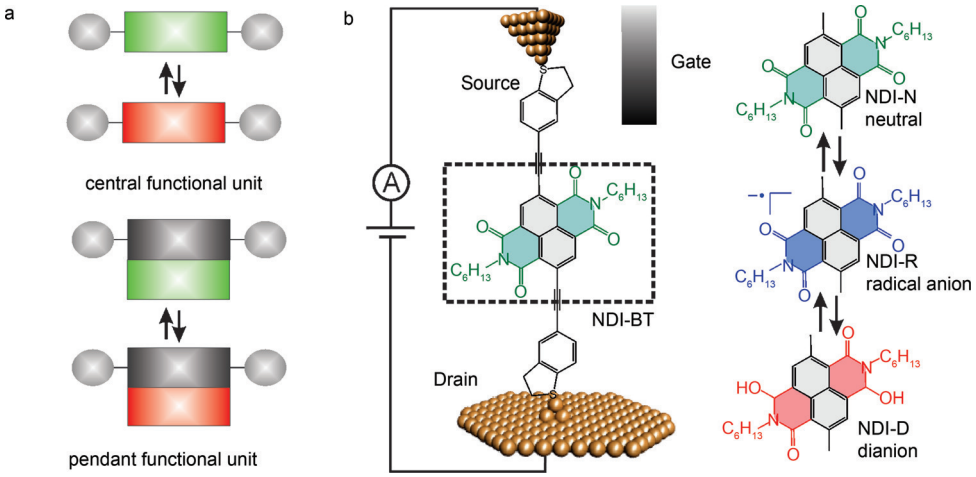

Figure 1. a) Schematic illustration of a single-molecule device with a central redox unit in the charge-transport pathway and a pendant redox unit. b) Schematic illustration of the electrochemically gated break junction experiment and molecular structure of NDI-BT in the neutral state (NDI-N), radical-anion state (NDI-R), and dianion state (NDI-D).

BT in THF. As the reduction of the NDI-BT to the dianion requires rather negative potentials, cyclic voltammetry (CV) and STM-BJ measurements were carried out in $HMImPF_6$ (1-hexyl-3-methylimidazolium hexafluorophosphate) in an oxygen-free environment. Compared to the electrochemical response of the bare Au(111)/$HMImPF_6$ interface (gray curve in Figure 2a), two pairs of reversible redox peaks appear in the voltammogram when the NDI-BT layer is present (black curve in Figure 2a). The first redox peak is located around −0.85 V versus Fc/Fc^+ and is attributed to the NDI-N/NDI-R redox process. The second redox peak is observed around −1.15 V versus Fc/Fc^+ and corresponds to the redox process of NDI-R to the NDI-D states.

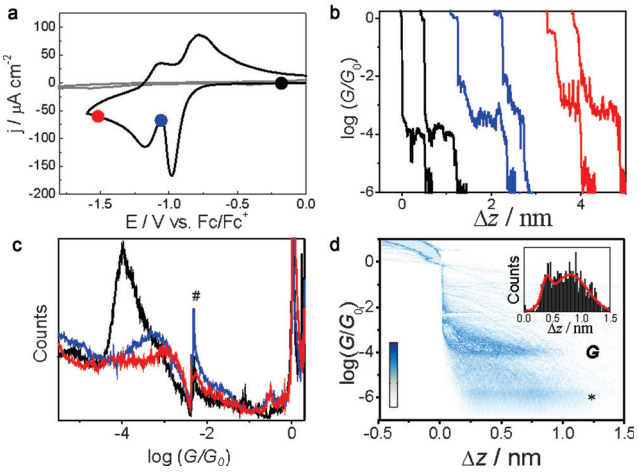

Figure 2. a) Cyclic voltammograms of NDI-BT immobilized on the Au(111) (black curve) and bare Au(111) (gray curve) in $HMImPF_6$. The scan rate was 50 $mV s^{-1}$. b) Typical conductance–distance traces of NDI-N (black), NDI-R (blue), and NDI-D (red). c) Conductance histogram sampled at different potential, # represents an artifact from the linear amplifier. d) Two-dimensional conductance–distance histogram of NDI-N, * represents the noise during the electrochemical STM BJ measurement. Inset: characteristic displacement histograms of NDI-N determined from the conductance region between $10^{-4.5}$ G_0 and 0.7 G_0.

The charge-transport properties of the single NDI-BT molecule were studied by STM-BJ measurements at room temperature. For further technical details can be found in our previous studies.[12] Figure 2b displays representative conductance (G) versus distance (Δz) traces measured at three different electrode potentials corresponding to NDI-N (black), NDI-R(blue), and NDI-D(red). Most of the curves show an initial conductance feature at G_0 with $G_0 = 2e^2/h = 77.5$ μS, which corresponds to the single gold–gold atomic conductance.[13] Subsequently, the conductance decreases abruptly ("jump out of contact"[14]) by several orders of magnitude. The plateaus at about 10^{-3}–10^{-4} G_0 are assigned to the conductance features of the single molecular NDI junctions, which strongly depend on the applied potential.

To provide a more quantitative comparison, 1000 individual conductance traces were sampled for each potential without any data selection. It was found that the conductance increased from 10^{-4} G_0 to $10^{-3.3}$ G_0 when the potential was swept from −0.20 V (NDI-N state) to −1.05 V versus Fc/Fc^+ (NDI-R state). Moreover, the NDI-D sampled at −1.50 V versus Fc/Fc^+ provided an even higher conductance of approximately $10^{-3.0}$ G_0. The on/off ratio from the NDI-N state to the NDI-D state is the conductance difference, which is around an order of magnitude, which is slightly larger than the previous studies on BDF and multiple state TTF switches,[4] and comparable with our recent single-molecule switch using an AQ redox unit.[6]

The two-dimensional conductance histogram[15] shown in Figure 2d provides direct access to the evolution of molecular junctions during the formation, stretching, and break-down steps. The high-density data cloud around $10^{-4.5}$ $G_0 \le G \le 10^{-3.5}$ G_0 represents the conductance range of the single NDI-N molecule bridging the gold electrodes. The inset in Figure 2d displays the characteristic displacement histograms[16] of NDI-N and shows that two peaks corresponding to tunneling and molecular junction in Figure 2d led to a junction formation probability of about 80%.

The reversibility of the switching process was also evaluated by continuous conductance switching between different charge states. As shown in Figure 3a, each conductance histogram is constructed from 1000 individual traces, and the applied potential changed per 1000 traces between −0.2 V (NDI-N), −1.05 V (NDI-R), and −1.5 V (NDI-D) versus Fc/Fc^+, respectively. It was found that NDI-BT can be switched forward and backward from NDI-N via NDI-R to the NDI-D state (1st–5000th traces), or switched between the NDI-N and NDI-R state (5000th to 7000th traces). These switching cycles suggest that the three charge

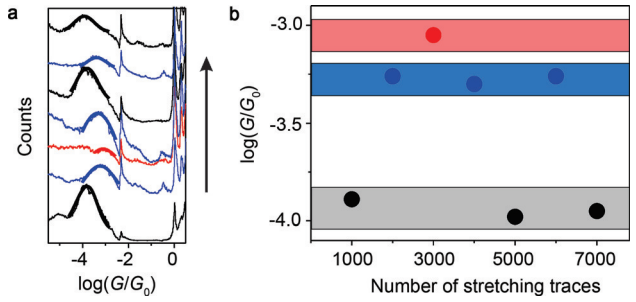

Figure 3. a) Conductance histogram constructed from 1000 individual traces of NDI-N (black), NDI-R (blue), and NDI-D (red). b) Most-probable conductance value determined from conductance histograms shown in (a).

states of the NDI molecule can be tuned reversibly by changing the applied potential even after more than 7000 stretching cycles (Figure 3b). The conductance peak became slight broader during the switching as a result of desorption of NDI-BT from the electrodes at a negative potential.[17]

To understand the observed switching mechanism between the three states of electrochemical gating we theoretically investigated the effect of the charge double layer on the conductance. The primary role of the charge double layer in our calculations is to control the number of electrons on the NDI molecule. To perform conductance calculations we used the Gollum[18] quantum transport code, with optimal gold-molecule-gold junction geometries and Hamiltonian matrix elements obtained using SIESTA.[19] To accurately describe single occupied levels of the NDI, all calculations were spin-polarized and the electron transmission coefficient function $T(E)$ calculated as the average of the spin-up and spin-down transmission coefficients. The three stages of gating are modeled with the three types of charge double layers (CDLs) shown in Figure 4 (the detailed junction and double layer geometries are shown in Figures S10–S12). To model the effect of gating, the distance (y) between the double layers and the plane of the molecule was adjusted such that the number of extra electrons on the molecule is 0, 1, and 2 for the neutral, radical anion, and dianion states, respectively. Figure 4a shows a negative charge double layer (the negative ions of the double layer lie closer to the plane of the NDI molecule) for which the NDI is neutral. Figure 4b,c show that positive charge double layers that attract electrons from the gold leads to the molecule, thereby creating the radical anion and dianion states.

To account for fluctuations in the charge double layer, the transmission coefficient and conductance were computed for different charge double layer arrangements, in which the anions and cations were randomly arranged at a fixed distance y. These were then averaged to yield the theoretical conductance G and transmission coefficient $T(E)$ as shown in Figure 4d–f (further details are given in the Supporting Information). Figure 4d–f show the average transmission coefficients for the three states. The conductances, which were computed from the transmission coefficients at the Fermi energy using the room temperature Landauer formula, show an increasing trend upon moving from the neutral state to the

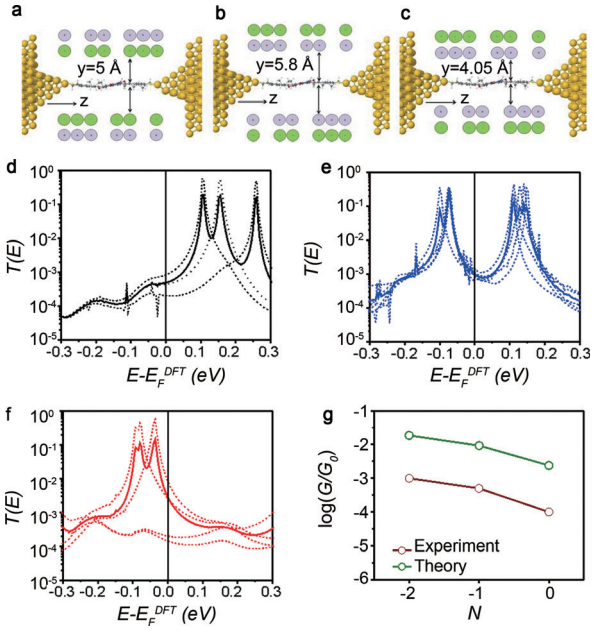

Figure 4. a–c) Junction geometries with charge double layers for the three states of electrochemical gating. a) The neutral state with negative-positive CDL that adjusts the molecular charge to zero. b,c) The radical anion and dianion states with positive-negative CDLs. d–f) Transmission curves for junction geometries with double layers located at distances $y = 5$ Å, $y = 5.8$ Å, and $y = 4.05$ Å shown in (a)–(c), respectively. The continuous curves are the averaged transmission coefficients and the dotted curves show the transmission coefficients for different charge double layer arrangements. The color code refers to the three different states, NDI-N (black), NDI-R (blue), and NDI-D (red). g) Comparison of the measured and computed averaged conductance values. The computed conductance values were calculated from the averaged transmission coefficient using the finite temperature Landauer formula (Eq. (1) in the Supporting Information) with a temperature of 300 K.

dianion state. In the radical anion state, the Fermi energy is trapped between two single electron resonances. This is apparent only in the spin-polarized calculation. In contrast, and as expected, the non-spin-polarized calculations give qualitatively different (and inaccurate) theoretical trends, because single-occupied orbitals are by definition located at the Fermi energy, and thereby result in an unphysical high conductance for the radical state (see Figure S7). Figure 4g illustrates that the electrochemical gating experiment consistently increases the conductance as the molecular charge goes from the neutral state to the dianion state. This trend agrees well with the theoretical charge-double-layer model, as Figure 4g illustrates. The theoretical conductance values are higher than the measured ones for all three states, which can be attributed to the neglect of environmental and thermal effects.[20] DFT is also known to underestimate the HOMO–LUMO gap, which results in an overestimated conductance.[14,16,21]

To conclude, we studied charge transport through an NDI single-molecule junction using an electrochemical STM-BJ technique and through ab initio simulations based on DFT. Benefiting from the wide potential window of the ionic liquid, we are able to access the three charge states of the NDI

molecule, which showed well-separated conductance features with an on/off ratio of around one order of magnitude between the most conductive NDI-R and the least conductive NDI-N state. The switching can be manipulated reversibly through the applied potential. Agreement between theory and experiment has been demonstrated by introducing a newly developed charge double layer model. The tristable charge states of the NDI molecule provide a unique opportunity beyond bistable on/off molecular switches, and lead to interesting logic gate and memory devices. More importantly, the comparable conductance changes between NDI molecules with pendent diimide units and with redox units integrated in molecular backbones suggests that the pendent redox unit can provide significant fine-tuning of single-molecule conductance triggered by external stimuli, in this case, an electrochemical gate. This offers great flexibility for the molecular design and synthesis of future molecular devices.

Acknowledgements

This work was generously supported by the National Natural Science Foundation of China and the Ministry of Science and Technology (via 973 project), the Swiss National Science Foundation (200020-144471), the EC FP7 ITN "MOLESCO" project number 606728, UK EPSRC grants EP/K001507/1, EP/J014753/1, EP/H035818/1. A.Q. also acknowledged the financial support from Ministry of Higher Education and Scientific Research, Al Qadisiyah University, IRAQ.

Keywords: break junction · electrochemical gating · molecular electronics · naphthalenediimide · single molecule studies

How to cite: *Angew. Chem. Int. Ed.* **2015**, *54*, 13586–13589
Angew. Chem. **2015**, *127*, 13790–13793

[1] a) A. C. Fahrenbach, C. J. Bruns, H. Li, A. Trabolsi, A. Coskun, J. F. Stoddart, *Acc. Chem. Res.* **2014**, *47*, 482–493; b) M. Irie, T. Fulcaminato, K. Matsuda, S. Kobatake, *Chem. Rev.* **2014**, *114*, 12174; c) B. L. Feringa, R. A. van Delden, N. Koumura, E. M. Geertsema, *Chem. Rev.* **2000**, *100*, 1789; d) P. Ceroni, A. Credi, M. Venturi, *Electrochemistry of Functional Supramolecular Systems*, Wiley-VCH, Weinheim, **2010**; e) E. Laviron, *J. Electroanal. Chem.* **1979**, *100*, 263; f) C. P. Andrieux, C. Blocman, J. M. Dumasbouchiat, J. M. Saveant, *J. Am. Chem. Soc.* **1979**, *101*, 3431.

[2] a) C. R. Arroyo, S. Tarkuc, R. Frisenda, J. S. Seldenthuis, C. H. M. Woerde, R. Eelkema, F. C. Grozema, H. S. J. van der Zant, *Angew. Chem. Int. Ed.* **2013**, *52*, 3152; *Angew. Chem.* **2013**, *125*, 3234; b) Z. Li, M. Smeu, S. Afsari, Y. Xing, M. A. Ratner, E. Borguet, *Angew. Chem. Int. Ed.* **2014**, *53*, 1098; *Angew. Chem.* **2014**, *126*, 1116; c) C. Huang, A. V. Rudnev, W. Hong, T. Wandlowski, *Chem. Soc. Rev.* **2015**, *44*, 889; d) C. Jia, J. Wang, C. Yao, Y. Cao, Y. Zhong, Z. Liu, Z. Liu, X. Guo, *Angew. Chem. Int. Ed.* **2013**, *52*, 8666; *Angew. Chem.* **2013**, *125*, 8828; e) C. Jia, B. Ma, N. Xin, X. Guo, *Acc. Chem. Res.* **2015**, *48*, 2565; f) R. M. Metzger, *Chem. Rev.* **2015**, *115*, 5056; g) C. Jia, X. Guo, *Chem. Soc. Rev.* **2013**, *42*, 5642.

[3] a) H. Tian, *Angew. Chem. Int. Ed.* **2010**, *49*, 4710; *Angew. Chem.* **2010**, *122*, 4818; b) J. E. Green, J. W. Choi, A. Boukai, Y. Bunimovich, E. Johnston-Halperin, E. DeIonno, Y. Luo, B. A. Sheriff, K. Xu, Y. S. Shin, H. R. Tseng, J. F. Stoddart, J. R. Heath, *Nature* **2007**, *445*, 414.

[4] a) N. J. Kay, S. J. Higgins, J. O. Jeppesen, E. Leary, J. Lycoops, J. Ulstrup, R. J. Nichols, *J. Am. Chem. Soc.* **2012**, *134*, 16817; b) E. Leary, S. J. Higgins, H. van Zalinge, W. Haiss, R. J. Nichols, S. Nygaard, J. O. Jeppesen, J. Ulstrup, *J. Am. Chem. Soc.* **2008**, *130*, 12204.

[5] Z. Li, H. Li, S. Chen, T. Froehlich, C. Yi, C. Schönenberger, M. Calame, S. Decurtins, S.-X. Liu, E. Borguet, *J. Am. Chem. Soc.* **2014**, *136*, 8867.

[6] M. Baghernejad, X. Zhao, K. Baruël Ørnsø, M. Füeg, P. Moreno-García, A. V. Rudnev, V. Kaliginedi, S. Vesztergom, C. Huang, W. Hong, P. Broekmann, T. Wandlowski, K. S. Thygesen, M. R. Bryce, *J. Am. Chem. Soc.* **2014**, *136*, 17922.

[7] X.-S. Zhou, L. Liu, P. Fortgang, A.-S. Lefevre, A. Serra-Muns, N. Raouafi, C. Amatore, B.-W. Mao, E. Maisonhaute, B. Schoellhorn, *J. Am. Chem. Soc.* **2011**, *133*, 7509.

[8] C. J. Lambert, *Chem. Soc. Rev.* **2015**, *44*, 875.

[9] a) F. Würthner, M. Stolte, *Chem. Commun.* **2011**, *47*, 5109; b) X. Zhan, A. Facchetti, S. Barlow, T. J. Marks, M. A. Ratner, M. R. Wasielewski, S. R. Marder, *Adv. Mater.* **2011**, *23*, 268; c) Z. Liu, G. Zhang, Z. Cai, X. Chen, H. Luo, Y. Li, J. Wang, D. Zhang, *Adv. Mater.* **2014**, *26*, 6965.

[10] A. J. Avestro, D. M. Gardner, N. A. Vermeulen, E. A. Wilson, S. T. Schneebeli, A. C. Whalley, M. E. Belowich, R. Carmieli, M. R. Wasielewski, J. F. Stoddart, *Angew. Chem. Int. Ed.* **2014**, *53*, 4442; *Angew. Chem.* **2014**, *126*, 4531.

[11] P. Moreno-García, M. Gulcur, D. Z. Manrique, T. Pope, W. Hong, V. Kaliginedi, C. Huang, A. S. Batsanov, M. R. Bryce, C. Lambert, T. Wandlowski, *J. Am. Chem. Soc.* **2013**, *135*, 12228.

[12] C. Li, I. Pobelov, T. Wandlowski, A. Bagrets, A. Arnold, F. Evers, *J. Am. Chem. Soc.* **2008**, *130*, 318.

[13] B. Q. Xu, N. J. J. Tao, *Science* **2003**, *301*, 1221.

[14] S. Y. Quek, M. Kamenetska, M. L. Steigerwald, H. J. Choi, S. G. Louie, M. S. Hybertsen, J. B. Neaton, L. Venkataraman, *Nat. Nanotechnol.* **2009**, *4*, 230.

[15] a) C. A. Martin, D. Ding, J. K. Sorensen, T. Bjornholm, J. M. van Ruitenbeek, H. S. J. van der Zant, *J. Am. Chem. Soc.* **2008**, *130*, 13198; b) A. Mishchenko, L. A. Zotti, D. Vonlanthen, M. Buerkle, F. Pauly, J. Carlos Cuevas, M. Mayor, T. Wandlowski, *J. Am. Chem. Soc.* **2011**, *133*, 184.

[16] W. Hong, D. Z. Manrique, P. Moreno-Garcia, M. Gulcur, A. Mishchenko, C. J. Lambert, M. R. Bryce, T. Wandlowski, *J. Am. Chem. Soc.* **2012**, *134*, 2292.

[17] J. D. C. Jacob, T. R. Lee, S. Baldelli, *J. Phys. Chem. C* **2014**, *118*, 29126.

[18] J. Ferrer, C. J. Lambert, V. M. Garcia-Suarez, D. Z. Manrique, D. Visontai, L. Oroszlany, R. Rodriguez-Ferradas, I. Grace, S. W. D. Bailey, K. Gillemot, H. Sadeghi, L. A. Algharagholy, *New J. Phys.* **2014**, *16*, 093029.

[19] J. M. Soler, E. Artacho, J. D. Gale, A. García, J. Junquera, P. Ordejón, D. Sánchez-Portal, *J. Phys. Condens. Matter* **2002**, *14*, 2745.

[20] M. Berritta, D. Z. Manrique, C. J. Lambert, *Nanoscale* **2015**, *7*, 1096.

[21] D. A. Egger, Z.-F. Liu, J. B. Neaton, L. Kronik, *Nano Lett.* **2015**, *15*, 2448.

Received: July 13, 2015
Published online: September 25, 2015

